3D face analysis from digital camera images

V. Patrangenaru, K. D. Yao, V. Balan

Abstract. In the present work, within the framework of 3D scenes analysis from digital camera images, we use the 8 point algorithm for 3D reconstruction of a landmarks configuration from their noncalibrated camera images, that leads to a 3D projective shape analysis. Our focus is on a two sample hypothesis testing method, for mean 3D projective shapes. The statistical analysis is performed for samples of pictures of 3D faces, without knowing *a priori* the distribution of such random 3D projective shapes, leading to a two sample test on the product of 3D projective spaces, that is simplified due to the Lie group structure of these object spaces.

M.S.C. 2010: 62H35, 94A08, 62H11, 62H10, 62H35.
Key words: RGB texture matching, projective shape, projective frame, eight points 3D reconstruction algorithm, hypothesis testing.

1 Introduction

The statistical analysis of projective shapes has been slowed down due to an overemphasized importance of similarity shape in image analysis, which was ignoring the basic principles of pinhole camera image acquisition, as well as due to insufficient dialogue between researchers in geometry, computer vision and statistical shape analysis. Projective shapes have been studied rather recently, and firstly, literature was bound to linear or 2D projective shape analysis, notable progress being provided in numerous works (e.g., [7, 5, 9, 4, 6, 3, 8]).

In this paper, within the framework of 3D projective shape analysis, we use the two sample hypothesis testing method for extrinsic means, as developed in [1, 10, 12], to differentiate between two faces, based on small samples of their digital camera images.

The mathematics background is basically developed on the space of 3D projective shapes of k-ads in general position $P\Sigma_3^k$, which is homeomorphic to $(\mathbb{R}P^3)^{k-5}$, and has a Lie group structure with the multiplication operation inherited from the quaternion multiplication on $S^3 \subset \mathbb{R}^4$. Therefore a 3D face analysis based on landmarks can

BSG Proceedings 23. The International Conference "Differential Geometry - Dynamical Systems" DGDS-2015, October 8-11, 2015, Bucharest-Romania, pp. 43-55.

make use of the recently developed nonparametric techniques for two sample tests on Lie groups (see [12, 10]). We emphasize that the reconstructed configuration of 3D landmarks obtained from pairs of noncalibrated camera images, is unique up to a projective transformation in 3D, as noticed in [11]; this allows to analyze without ambiguity the projective shapes of such configurations (see [11]). The developed statistical analysis is performed for samples of pictures of faces, without making any distributional assumption for the corresponding 3D projective shapes of human facial surfaces. We provide, as well, a brief description of the methodology used, which can be found in detail in [10].

2 Projective shape space of 3D configurations

Our statistical analysis will be done on the 3D projective shape space $P\Sigma_3^k \simeq (\mathbb{R}P^3)^{k-5}$. The manifold structure of this space will allow us to use the *asymptotic theory for means on manifolds*.

Furthermore this space has an additional structure of a Lie group, which is of great use when dealing with unmatched pairs of data.

For each 3D objects in our data sample, we focus on the configuration of the 3D coordinates of our landmarks. We say that two such configurations of labeled points in $\mathbb{R}^3$ have *the same projective shape* if they differ by a *projective transformation* of $\mathbb{R}^3$.

Generally, a projective transformation ν of $\mathbb{R}^m$ is defined in terms of a matrix $A = (a_i^j) \in GL(m+1, \mathbb{R})$, via $\nu(x^1, \ldots, x^m) = (y^1, \ldots, y^m)$,

$$y^j = \frac{\sum_{i=1}^m a_i^j x^i + a_{m+1}^j}{\sum_{i=1}^m a_i^{m+1} x^i + a_{m+1}^{m+1}}, \ \forall j = 1, \ldots, m. \tag{2.1}$$

However, in applications, such projective transformations act only on subsets of $\mathbb{R}^m$ and consequently they do not have a group structure under composition. Recall that $\mathbb{R}P^m$ is the set of equivalence classes of points in $\mathbb{R}^{m+1}\backslash\{0\}$, where two points x, y are equivalent if there is a $\lambda \in \mathbb{R}\backslash 0$, with $y = \lambda x$. We will use the notation $[x]$ with $x \in \mathbb{R}^{m+1}\backslash\{0\}$ to represent the equivalence class of $x = (x^1, \ldots, x^{m+1})$, which is also written as $[x^1 : x^2 : \cdots : x^{m+1}]$, featuring the *homogeneous coordinates* $(x^1, \ldots, x^{m+1})$ of $[x]$, which are unique up to a nonzero multiplicative constant. Note that since $\mathbb{R}^m$ can be identified with an open affine subset of $\mathbb{R}P^m$, any configuration in $\mathbb{R}^m$ can be regarded as a configuration in $\mathbb{R}P^m$ and the pseudo-action by the projective transformations on open dense subsets of $\mathbb{R}^m$ can be extended to a group action of the projective group $PGL(m)$, which has the form $\alpha: \ PGL(m) \times \mathbb{R}P^m \to \mathbb{R}P^m$,

$$\alpha([A], [x]) = [Ax], \ \ \forall \ A \in GL(m+1, \mathbb{R}) \ , \ \forall \ x \in \mathbb{R}^{m+1}.$$

Therefore, rather than considering projective shapes of configurations in $\mathbb{R}^m$, we consider projective shapes of configurations in the projective space $\mathbb{R}P^m$. If one multiplies the matrix A by a nonzero constant, then the equation (2.1) does not change; therefore the group $PGL(m)$ of projective transformations of $\mathbb{R}^m$ has dimension $(m+1)^2 - 1 = m(m+2)$. Thus, a projective transformation is determined by its values on $m+2$ points in general position.

Definition 2.1. A *projective frame* in $\mathbb{R}P^m$ is an ordered set of $m+2$ projective points in general position.

An example of projective frame in $\mathbb{R}P^m$ is the *standard projective frame*

$$([e_1], \ldots, [e_{m+1}], [e_1 + ... + e_{m+1}]).$$

In projective shape analysis it is preferable to employ coordinates invariant with respect to the group PGL(m). A projective transformation takes a projective frame to a projective frame, and its action on $\mathbb{R}P^m$ is determined by its action on a projective frame; therefore, if we define the *projective coordinate(s)* of a point $p \in \mathbb{R}P^m$ w.r.t. a projective frame $\pi = (p_1, \ldots, p_{m+2})$ as being given by

$$p^\pi = \beta^{-1}(p),$$

where $\beta \in PGL(m)$ is a projective transformation taking the standard projective frame to π, these coordinates have automatically the invariance property.

Definition 2.2. A *projective shape* of a k-ad (configuration of k labeled points) is the orbit of that k-ad under projective transformations. If the k-ad is regarded as a point on $(\mathbb{R}P^m)^k$, then such a transformation acts at the same time on each point of the k-ad; therefore the action of PLG(m) is the diagonal action of this group on $(\mathbb{R}P^m)^k$,

$$\alpha_k(p_1, ..., p_k) = (\alpha(p_1), ..., \alpha(p_k))$$

The m-dimensional projective shape space of a *generic k-ad* is determined by the *projective coordinates* $(p^\pi_{m+3}, ..., p^\pi_k)$ of $k-m-2$ of its points, relative to other $(m+2)$ of its points that form a projective frame. The set $P\Sigma^k_m$ of projective shapes of generic k-ads including a projective frame at given labels, is therefore isomorphic to $(\mathbb{R}P^m)^{k-m-2}$ [11]; keeping this identification in mind, from this point on, we will use the symbol $P\Sigma^k_m$, when referring to the projective shape space $P\Sigma^k_m$.

2.1 Homogeneous spaces and the Lie group structure of $(\mathbb{R}P^3)^q$

Let $\tilde{\alpha} : \mathcal{G} \times \mathcal{M} \to \mathcal{M}$ be a *left action* of the group $(\mathcal{G}, \odot)$ on $\mathcal{M}$, and let $\tilde{\alpha}_k : \mathcal{M} \to \mathcal{M}$, be given by $\tilde{\alpha}_k(x) := \tilde{\alpha}(k, x)$. Recall that the left action $\tilde{\alpha}$ is called *transitive* if for all $x, x' \in \mathcal{M}$, there exists $k \in \mathcal{G}$ such that $\tilde{\alpha}_k(x) = x'$. Also recall that the *orbit* $\mathcal{G}(x)$ *of a point* $x \in \mathcal{M}$ is the set $\{\tilde{\alpha}(k, x), k \in \mathcal{G}\}$. The space $\mathcal{M}$ is called $\mathcal{G}$*-homogeneous space* if there exists a point x such that $\mathcal{G}(x) = \mathcal{M}$. In the case $\mathcal{M}$ is a manifold, we assume in addition that $(\mathcal{G}, \odot)$ is a Lie group and the action $\tilde{\alpha}$ is smooth. A Lie group $(\mathcal{G}, \odot)$ is automatically a $\mathcal{G}$-homogeneous space, for the action $\tilde{\alpha} = \odot$.

In Statistics it makes sense to consider the equality of means on a smooth object space $\mathcal{M}$, with an action of a Lie group $\mathcal{G}$, only for means that lie on the same orbit, and for this reason, all the smooth object spaces considered so far are homogeneous spaces (see [10], Chapter 3). A notable example of such an object space is the space $\mathbb{R}P^m$, *space of axes* in $\mathbb{R}^{m+1}$, with the group action is given by $\alpha : PGL(m) \times \mathbb{R}P^m \to \mathbb{R}P^m$

$$\alpha([A], [x]) = [Ax], \ \ \forall\ A\ \in GL(m+1, \mathbb{R}),\ \forall\ x \in \mathbb{R}^{m+1}.$$

In particular the 3D real projective space $\mathbb{R}P^3$ is a homogeneous space. However, in addition, $\mathbb{R}P^3$ can be identified with the quotient space $S^3/\{x,-x\}$, and with this representation, it follows that the operation

$$[x]\odot[y]=[x\cdot y]\quad for\quad [x],[y]\ \in\mathbb{R}P^3,$$

where $\cdot$ is the quaternion multiplication on S^3, is a well defined Lie group multiplication on $\mathbb{R}P^3$ [1]. Also for $[p]=[x:y:z:t]\ \in\mathbb{R}P^3$, its conjugate is $[\bar{p}]=[-x:-y:-z:t]\in\mathbb{R}P^3$, the inverse map on $\mathbb{R}P^3$ is given by

$$[p]^{-1}=\|(x,y,z,t)\|^{-2}[\bar{p}],$$

and the identity of this Lie group is $1_{\mathbb{R}P^3}=[0:0:0:1]$. Using the same representation of elements of $\mathbb{R}P^3$, the projective shape space $(\mathbb{R}P^3)^q$, $(q=k-5)$ inherits a Lie group structure from the group structure of $\mathbb{R}P^3$.

3 Two sample means tests for unmatched pairs on a Lie group

Given that $(\mathbb{R}P^3)^q$ has a Lie group structure, and a Lie group is a homogeneous manifold with a simply transitive Lie group action, in this section we derive the large sample distribution of the tangential component of the mean change between the extrinsic sample means of two random objects on an embedded Lie group $\mathcal{M}$, which is needed in the two sample problem for means of unmatched pairs on such a Lie group.

Let $\mathcal{M}$ be a $\mathcal{G}$-homogeneous space, where $\mathcal{M}$ is an embedded manifold and $(\mathcal{G},\odot)$ a Lie group that acts simply transitively on $\mathcal{M}$ via a smooth left action $\alpha:\mathcal{G}\times\mathcal{M}\to\mathcal{M}$. For $a=1,2$, let $X_{a,1},\cdots,X_{a,n_a}$ be independent random samples defined on $\mathcal{M}$, from a distribution Q_a, with the extrinsic means $\mu_{1,j},\mu_{2,j}$ and with the corresponding extrinsic covariance matrices $\Sigma_{1,j},\Sigma_{2,j}$, where $j:\mathcal{M}\to\mathbb{R}^N$ is the embedding. Then, a two-sample hypothesis testing problem can be formulated as follows

$$H_0:\mu_{1,j}=\alpha(\delta,\mu_{2,j})\quad\text{vs.}\quad H_1:\mu_{1,j}\neq\alpha(\delta,\mu_{2,j}),$$

for $\delta\in\mathcal{G}$. Now for a fixed object $\mu_{2,j}$ the mapping $\alpha^{\mu_{2j}}:\mathcal{G}\to\mathcal{M},\quad \alpha^{\mu_{2j}}(g)=\alpha(g,\mu_{2j}),\ \forall\ g\in\mathcal{G}$ is one-to-one, and we can now rewrite the hypothesis problem from above as follows

$$H_0:(\alpha^{\mu_{2,j}})^{-1}(\mu_{1,j})=\delta\quad\text{vs.}\quad H_1:(\alpha^{\mu_{2,j}})^{-1}(\mu_{1,j})\neq\delta. \tag{3.1}$$

If in addition $\mathcal{G}$ acts simply transitively on $\mathcal{M}$, we further define the smooth map $H:\mathcal{M}^2\to\mathcal{G}$ by $H(x_1,x_2)=(\alpha^{x_2})^{-1}(x_1)$, whose asymptotic behavior involving $H(\bar{X}_{n_1,j},\bar{X}_{n_2,j})$ has been addressed in [12]. In the case of a Lie group $(\mathcal{G},\odot)$ consider the particular case of (3.1) null hypothesis

$$H_0:\ \mu_{1,j}=\mu_{2,j}\odot\delta\quad\text{vs.}\quad H_1:\ \mu_{1,j}\neq\mu_{2,j}\odot\delta. \tag{3.2}$$

Since for $a=1,2,X_{a,1},\ldots,X_{a,n_a}$ *independent and identically distributed* (i.i.d.) random objects on $\mathcal{G}$, we can rewrite the hypothesis in (3.2) as follows

$$H_0:\ \mu_{2,j}^{-1}\odot\mu_{1,j}=\delta\quad\text{vs.}\quad H_1:\ \mu_{2,j}^{-1}\odot\mu_{1,j}\neq\delta.$$

3.1 Asymptotic behavior and nonparametric bootstrap

We are led into characterizing the asymptotic behavior of $\bar{X}_{2,j}^{-1} \odot \bar{X}_{1,j}$, where $\bar{X}_{1,j}, \bar{X}_{2,j}$ are the sample extrinsic mean estimators corresponding to the two random samples.

For $a = 1, 2$, let $X_{a,1}, \cdots, X_{a,n_a}$ be independent random samples defined on the m dimensional Lie group $\mathcal{G}$, from a distribution Q_a, with the extrinsic means $\mu_{1,j}, \mu_{2,j}$ and the corresponding extrinsic covariance matrices $\Sigma_{1,j}, \Sigma_{2,j}$. Let $j : \mathcal{G} \to \mathbb{R}^N$ be an embedding. We are interested in the asymptotic behavior of

$$\tan_{j(\mu_{2,j}^{-1} \odot \mu_{1,j})} \left(j(\bar{X}_{2,j}^{-1} \odot \bar{X}_{1,j}) - j(\mu_{2,j}^{-1} \odot \mu_{1,j}) \right).$$

Recall that the map $(g_1, g_2) \to g_1 \odot g_2$, for $g_1, g_2 \in \mathcal{G}$ is a smooth map from $\mathcal{G} \times \mathcal{G} \to \mathcal{G}$. Therefore, the asymptotic distribution, follows from a more general case, involving manifolds $\mathcal{M}$ and $\mathcal{N}$, along with their corresponding embeddings $j_1 : \mathcal{M} \to \mathbb{R}^{N_1}$ and $j_2 : \mathcal{N} \to \mathbb{R}^{N_2}$.

Theorem 3.1. *For $a = 1, 2$ let $X_{a,1}, \cdots, X_{a,n_a}$ be independent random samples defined on $\mathcal{G}$, from the j-nonfocal distributions Q_a, with the extrinsic means $\mu_{a,j}$ and the extrinsic covariance matrices $\Sigma_{a,j}$. Also, let $n = n_1 + n_2$ such that $n_1/n \to \pi \in (0, 1)$, as $n_a \to \infty$. Then we have the following*

$$n^{1/2} \ \tan_{j(\mu_{2,j}^{-1} \odot \mu_{1,j})} \left(j(\bar{X}_{2,j}^{-1} \odot \bar{X}_{1,j}) - j(\mu_{2,j}^{-1} \odot \mu_{1,j}) \right) \to_d N_m(0_m, \Sigma_j^{\iota G}), \tag{3.3}$$

where $\Sigma_j^{\iota G}$ is linear as a function of the extrinsic covariance matrices $\Sigma_{1,j}, \Sigma_{2,j}$. In particular, under the null hypothesis of (3.1), we have the following

$$n^{1/2} \ \tan_{j(\mu_{2,j}^{-1} \odot \mu_{1,j})} \left(j(\bar{X}_{2,j}^{-1} \odot \bar{X}_{1,j}) - j(\delta) \right) \to_d N_m(0_m, \Sigma_j^{\iota G})$$

and in case $\Sigma_j^{\iota G}$ is positive definite, we get

$$\begin{aligned} n(\tan_{j(\mu_{2,j}^{-1} \odot \mu_{1,j})}(j(\bar{X}_{2,j}^{-1} \odot \bar{X}_{1,j}) - j(\delta)))^T)(\Sigma_j^{\iota G})^{-1} \\ (\tan_{j(\mu_{2,j}^{-1} \odot \mu_{1,j})}(j(\bar{X}_{2,j}^{-1} \odot \bar{X}_{1,j}) - j(\delta))) \to_d \chi_m^2. \end{aligned}$$

In applications, we often have unknown distributions Q_a, $a = 1, 2$, and the samples are small; in such case we may use a nonpivotal bootstrap methodology for the two sample problem H_0.

Theorem 3.2. *Under the hypotheses of Theorem 3.1, assume in addition that for $a = 1, 2$ the support of the distribution of $X_{a,1}$ has an absolutely continuous component and finite moments of sufficiently high order. Then the distribution of*

$$n^{1/2} \ \tan_{j(\mu_{2,j}^{-1} \odot \mu_{1,j})} \left(j(\bar{X}_{2,j}^{-1} \odot \bar{X}_{1,j}) - j(\mu_{2,j}^{-1} \odot \mu_{1,j}) \right)$$

can be approximated by the bootstrap distribution of

$$n^{1/2} \ \tan_{j(\bar{X}_{2,j}^{-1} \odot \bar{X}_{1,j})} \left(j(\overline{X^*}_{2,j}^{-1} \odot \overline{X^*}_{1,j}) - j(\bar{X}_{2,j}^{-1} \odot \bar{X}_{1,j}) \right),$$

with an error $O_p(n^{-1/2})$, where, for $a = 1, 2, \overline{X^*}_{a,j}$ is the extrinsic mean of the bootstrap resamples X^*_{a,j_a}, $j_a = 1, ..., n_a$, given X_{a,j_a}, $j_a = 1, ..., n_a$.

3.2 Two sample tests for VW-means of unmatched pairs of 3D projective shapes

The real projective space $\mathbb{R}P^m$ is embedded in the space of $(m+1)\times(m+1)$ positive semi-definite symmetric matrices, via the Veronese-Whitney (VW) map $j_1 : \mathbb{R}P^m \to S_+(m+1,\mathbb{R})$ given by

$$j_1([x]) = xx^T, \|x\| = 1.$$

Let $q = k-m-2$. One defines as the VW embedding j_q of the projective shape space $(\mathbb{R}P^m)^q$, $j_q : (\mathbb{R}P^m)^q \to (S(m+1))^q$ via

$$j_q(([x_1],\ldots,[x_q])) = (j_1([x_1]),\ldots,j_1([x_q]),$$

with $x_s \in \mathbb{R}^{m+1},\ x_s^T x_s = 1,\ s = 1,\ldots,q$.

Human and machine vision are 3D projective shape based [11]. In the case of the 3D projective shape space of k-ads $q = k-5$, therefore, for a statistical analysis of 3D projective shapes, we are lead into considering random objects (r.o.'s) Y on $(\mathbb{R}P^3)^q$ that have a VW-mean (have an extrinsic mean w.r.t. the VW-embedding j_q). The probability measure P_Y on $(\mathbb{R}P^3)^q$, associated with such a r.o. is said to be *VW-nonfocal probability measure* on $(\mathbb{R}P^3)^q$. The VW-mean of a VW-nonfocal the probability measure $P_Y, Y = ([X^1],...,[X^q]),\quad (X^s)^T X^s = 1,\ \forall\, s = 1,\ldots,q$, is given by

$$\mu_{j_q} = (\gamma_1(4),\ldots,\gamma_q(4)),$$

where $(\lambda_s(a),\gamma_s(a))$, $a = 1,2,3,4$ are the eigenvalues in increasing order, and the corresponding unit eigenvectors of the matrix $E[X^s(X^s)^T]$, respectively (see [11], [6]). In particular, given a random sample of 3D projective shapes $y_1,\ldots,y_n$, with $y_i = [x_i], x_i^T x_i = 1, \forall i = 1,\ldots,n$, their sample VW-mean is

$$\bar{y}_{j_q} = (g_1(4),\ldots,g_q(4)),$$

where $(\hat{\lambda}_s(a), g_s(a))$, $a = 1,2,3,4$ are the eigenvalues in increasing order, and the corresponding unit eigenvectors of the matrix

$$\frac{1}{n}\sum_{i=1}^{n} x_i x_i^T.$$

For $a = 1,2$, let $\{Y_{a,r}\}_{r=1}^{n_a}$ be i.i.d. r.o's defined on $(\mathbb{R}P^3)^q$ from independent VW-nonfocal distributions $\mathcal{Q}_a$.
Assume $n = n_1 + n_2$ and $\lim_{n\to\infty} \frac{n_1}{n} \to \pi \in (0,1)$. Let φ be the affine chart defined on an affine open neighborhood of $1_{\mathbb{R}P^3}$, given by $\varphi([(x^0,x^1,x^2,x^3)^T]) = (\frac{x^1}{x^0}, \frac{x^1}{x^0}, \frac{x^1}{x^0})$, and define the chart φ_q on an open neighborhood of $1_{(\mathbb{R}P^3)^q}$, given by

$$\varphi_q([x_1],\ldots,[x_q]) = (\varphi([x_1]),\ldots,\varphi([x_q])).$$

Then from Theorem 3.2, for $\delta = 1_{(\mathbb{R}P^3)^q}$, under H_0, the distribution of

$$D = \varphi_q(\bar{Y}_{n_2,j_q}^{-1} \otimes \bar{Y}_{n_1,j_q})$$

can be approximated by the bootstrap joint distribution of

$$D^\star = \varphi_q(\bar{Y^\star}^{-1}_{n_2,j_q} \otimes \bar{Y}^\star{}_{n_1,j_q}),$$

with an error of order $O_P(n^{-1/2})$.

We can construct a nonparametric bootstrap confidence region of size $1-\alpha$ for $\mu^{-1}_{2,j_q} \otimes \mu_{1,j_q}$, for simplicity by using simultaneous confidence intervals. We will then expect to *fail to reject* the null hypothesis, if we have 0 in all of our simultaneous confidence intervals for all the affine coordinates.

4 Data set and hypothesis testing results

The analyzed data set consists of images of faces:

Figure 1: Faces used for analysis

For analysis, ten landmarks were placed, resulting 3D projective shapes of k-ads ($k = 10$).

The collections and reconstructions of all of our landmark configurations were done in Matlab. The landmarks are shown below:

Figure 2: Landmark placements for all faces

The first five landmarks were used as projective frame, which are, in increasing order: *Pronasale, right and left Endocathion, Labiale Superius, left Crista Philtri.*

Comparing male faces. For our result we used the simultaneous confidence intervals mentioned above. We failed to reject the null hypothesis

$$H_0 : \mu^{-1}_{2,j_5} \odot \mu_{1,5} = 1_{(\mathbb{R}P^3)^5}$$

if all of our confidence intervals contain the value 0. For this two sample test, we use the following two data sets:

Figure 3: Images of two male faces

Bootstrap marginals and simultaneous confidence intervals (male faces).

Simultaneous confidence intervals for changes between the 2 mean projective shapes of the two faces landmarks 6 to 8			
	LM6	LM7	LM8
x	$(-1.111498, 0.805386)$	$(-1.117512, 1.099536)$	$(-1.296547, 0.966296)$
y	$(-1.215218, 0.710931)$	$(-1.355167, 1.336021)$	$(-0.635282, 1.372627)$
z	$(-1.161234, 1.150762)$	$(-1.432217, 1.349541)$	$(-1.394141, 1.349442)$

Simultaneous confidence intervals for changes between the 2 mean projective shapes of the two faces landmarks 9 and 10		
	LM9	LM10
x	$(0.952164, 0.996354)$	$(-0.962541, 1.005917)$
y	$(-0.760124, 1.129782)$	$(-1.070631, 0.982195)$
z	$(-0.817503, 1.319117)$	$(-1.319374, 1.089272)$

We notice that one of the simultaneous confidence intervals for landmark 9, corresponding to the right *Exocanthion*, does not contain 0. We then reject the null hypothesis, showing that there is significant projective shape change between the two male faces.

Comparing male and female faces. To get the simultaneous confidence intervals for our null hypothesis $H_0 : \mu_{1,j_5}^{-1} \odot \mu_{2,j_5} = 1_{(\mathbb{R}P^3)^5}$, we use the image from below as input data:

Bootstrap marginals and simultaneous confidence intervals for cross gender analysis.

Simultaneous confidence intervals for cross gender landmarks 6 to 8			
	LM6	LM7	LM8
x	$(-1.251984, 1.202986)$	$(-1.228628, 1.234229)$	$(-1.273092, 1.332798)$
y	$(-0.633834, 0.902621)$	$(-0.928523, 0.995304)$	$(-0.226587, 0.865510)$
z	$(-0.231190, 0.432009)$	$(-0.684483, 1.045302)$	$(-0.590623, 1.132418)$

Simultaneous confidence intervals for cross gender landmarks 9 and 10		
	LM9	LM10
x	$(0.998446, 1.028374)$	$(-0.988191, -0.931250)$
y	$(-0.702335, 0.540613)$	$(-1.162803, 1.008259)$
z	$(-1.057821, 0.849069)$	$(-0.118635, 0.969739)$

Figure 4: Female Sample

Figure 5: Male 2 Sample

The landmarks 9 and 10 corresponding to the right and left Exocanthion have intervals not containing 0. We reject the null hypothesis, and conclude that there is a significant projective shape change between the two faces.

Cross validation. We separate the original sample in figure 5 into two smaller data sets of pairs of pictures of sizes $n_1 = 5$ and $n_2 = 6$. They are displayed below:

Bootstrap axial marginals and simultaneous confidence regions for cross validation.

Simultaneous confidence interval for cross validation face 2 for landmarks 6 to 8			
	LM6	LM7	LM8
x	$(-17.496785, 3.552070)$	$(-4.027879, 4.860970)$	$(-1.990796, 7.497709)$
y	$(-10.967285, 4.340129)$	$(-3.776026, 9.830274)$	$(-7.558584, 0.865119)$
z	$(-2.724184, 13.093615)$	$(-3.006049, 5.891478)$	$(-0.698745, 4.293201)$

Simultaneous confidence intervals for cross validation face 2 for landmarks 9 and 10		
	LM9	LM10
x	$(-2.459882, 1.230096)$	$(-3.264292, 1.036499)$
y	$(-1.631839, 0.983147)$	$(-1.387133, 2.942318)$
z	$(-1.451487, 1.196335)$	$(-0.916768, 1.658124)$

All the simultaneous intervals (affine coordinates) contain 0. We fail to reject the null hypothesis; there no statistically significant mean projective shape change, as expected.

5 Landmark coordinates from ideal noncalibrated camera images

Our data sets are formed of digital camera images of faces. The 3D face analysis we are conducting is a landmark based analysis. Our landmarks are composed of reconstructed 3D points in a particular configuration.

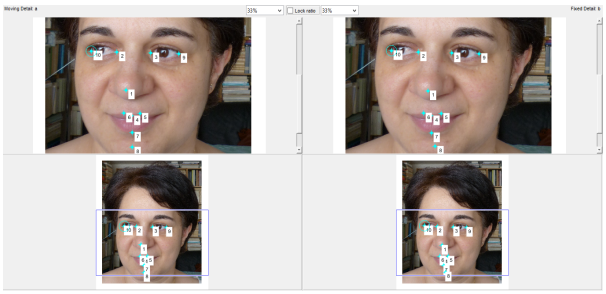

Figure 6: Landmark placements in Matlab

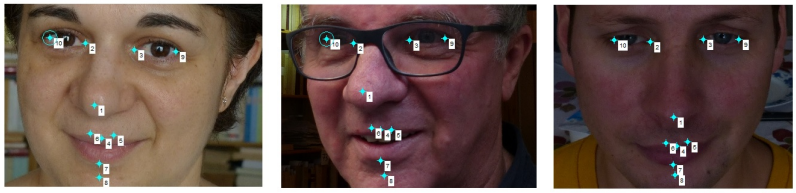

Figure 7: Landmark placements for three data samples

5.1 Matlab data set

The collection of our landmarks in Matlab is done in a few stages. For any one reconstruction of a particular 3D object (faces, flowers, leaves, etc...), two pictures from two different angles are needed. Once the pair of pictures is stored and saved in the an appropriate window within the Matlab platform, the digital images are loaded using the **imread** command in Matlab. The landmarks are manually selected using the function **cpselect()**. We illustrate a set of landmarks in figure 6.

Generally, a finite configuration of eight or more points in general position in 3D can be reconstructed, by using the fundamental matrix of the coordinates of the images of these points provided by two ideal noncalibrated digital camera views (see [2]). We assign the same landmarks throughout our whole data sample; the images in figure 7 show the placement of our matching points.

By this method we usually get reliable 3D coordinates for our landmarks. However, one drawback associated with this technique is that it is hard to visualize the reconstructed 3D configurations. In fact, getting a decent visualization of our reconstruction may require the collection of a large amount of landmarks, which can be time consuming.

To illustrate this particular situation we have the following 3D reconstruction involving 80 landmarks placed on a pair of pictures of an oak leaf and resulting in the following 3D images without color and/or texture.

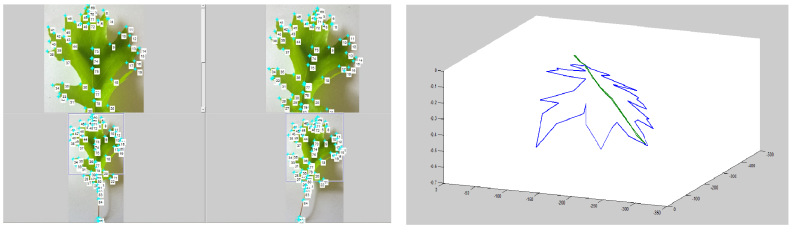

Figure 8: Oak leaf reconstruction with midriff

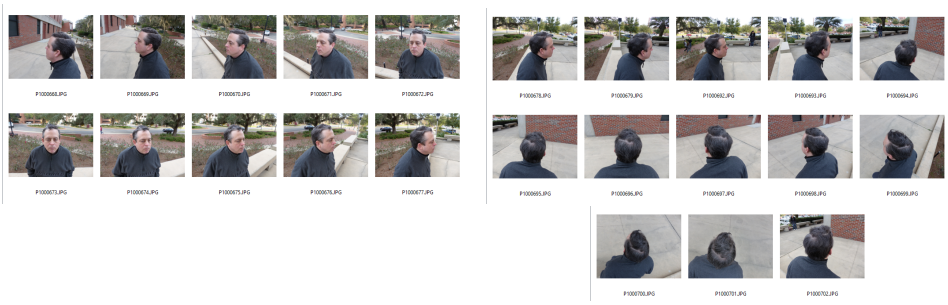

Figure 9: Pictures used for 3D reconstruction

5.2 New directions in 3D data collection methods from digital camera outputs

Recently for our data analysis we started using a professional version of Agisoft, which extracts the 3D image of a surface from two or more non-calibrated digital camera views, based on RGB texture matching followed by a 3D reconstruction algorithm. This software gives us a much better visualization of our reconstructed data set without relying on landmark collection and the use of an eight point algorithm to estimate the fundamental matrix.

Although the reconstruction of the midface could be done with just two uncalibrated camera images, we get a better resolution and complete reconstruction of the surface of a head or face, by increasing the number of images of the same individual. We illustrate this fact we use set of pictures in Fig. 9. After the reconstruction is done, we may visualize our result and also indicate the relative camera placement in Fig. 10. The Agisoft output then gives us the 3D coordinates of our ten landmarks in Figs. 11-12.

Acknowledgement. The authors are indebted to Vlad P. Patrangenaru for introducing them to Agisoft. The first two authors are also grateful to the National Security Agency for award NSA-MSP-H98230-15-1-0227 and to the National Science Foundation for award NSF-DMS-1106935.

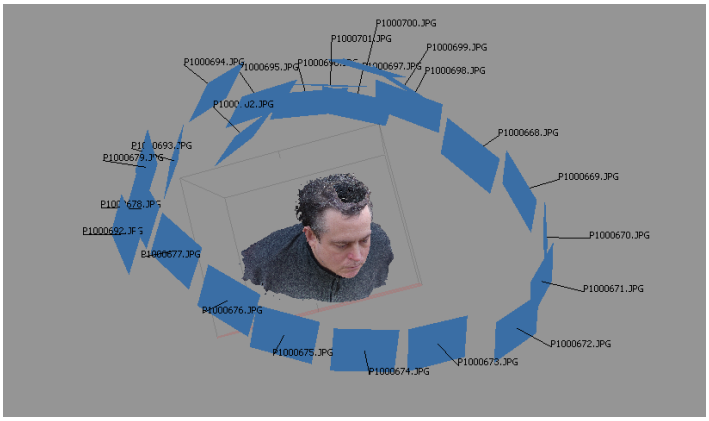

Figure 10: 3D Face reconstruction with camera placement

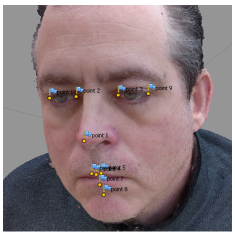

	X est	Y est	Z est
point 1	-0.056717	-0.181218	0.342859
point 2	-1.545557	-1.970076	3.936616
point 3	1.577311	-2.008529	4.018979
point 4	0.103276	2.888047	1.164003
point 5	0.478865	2.788800	1.214435
point 6	-0.224090	2.844635	1.227195
point 7	0.228277	3.734438	1.206160
point 8	0.288231	4.821007	1.547070
point 9	3.685678	-1.958006	4.334273
point 10	-3.676733	-1.767309	4.242580

Figure 11: Landmark placement and coordinates

Figure 12: Pictures for 3D reconstructions

References

[1] M. Crane, V. Patrangenaru, *Random change on a Lie group and mean glaucomatous projective shape change detection from stereo pair image*, Journal of Multivariate Analysis **102** (2011), 225-237.

[2] R. Hartley and A. Zisserman, *Multiple View Geometry in Computer Vision*, 2-nd edition, Cambridge University Press, 2004.

[3] J. T. Kent, K. V. Mardia, *A new representation for projective shape*, in (Eds: S. Barber, P. D. Baxter, K. V.Mardia & R. E. Walls) "Interdisciplinary Statistics and Bioinformatics", Leeds, Leeds University Press 2006, 75–78; http://www.maths.leeds.ac.uk/lasr2006/proceedings/

[4] J.L. Lee, R. Paige, V. Patrangenaru, F. Ruymgaart, *Nonparametric density estimation on homogeneous spaces in high level image analysis*, in (Eds: R. G. Aykroyd, S. Barber, & K. V. Mardia) "Bioinformatics, Images, and Wavelets", Department of Statistics, University of Leeds 2004, 37–40; http://www.maths.leeds.ac.uk/Statistics/workshop/leeds2004/temp

[5] K. V. Mardia, C. Goodall, A. N. Walder, *Distributions of projective invariants and model based machine vision*, Adv. in App. Prob. **28** (1996), 641–661.

[6] K. V. Mardia and V. Patrangenaru, *Directions and projective shapes*, Annals of Statistics **33** (2005), 1666–1699.

[7] S. J. Maybank, *Classiffication based on the cross ratio*, in "Applications of Invariance in Computer Vision", Lecture Notes in Comput. Sci. 825 (Eds: J.L. Mundy, A. Zisserman and D. Forsyth), Springer, Berlin 1994, 433–472.

[8] A. Munk, R. Paige, J. Pang, V. Patrangenaru, F. H. Ruymgaart, *The one and multisample problem for functional data with applications to projective shape analysis*, J. of Multivariate Anal. **. 99** (2008), 815–833.

[9] V. Patrangenaru, *New large sample and bootstrap methods on shape spaces in high level analysis of natural images*, Commun. Statist. **30** (2001), 1675–1693.

[10] V. Patrangenaru and L. Ellingson, *Nonparametric Statistics on Manifolds and Their Applications to Object Data Analysis*, CRC-Chapman & Hall. 2015.

[11] V. Patrangenaru, X. Liu and S. Sugathadasa, *Nonparametric 3D projective shape estimation from pairs of 2D images - I, In memory of W.P. Dayawansa*, Journal of Multivariate Analysis **101** (2010), 11–31.

[12] V. Patrangenaru, M. Qiu and M. Buibas, *Two sample tests for mean 3D projective shapes from digital camera images*, Methodology and Computing in Applied Probability **16** (2014), 485–506.

Authors' addresses:

Vic Patrangenaru and Kouadio David Yao
Florida State University, Tallahassee, FL, USA.
E-mail: vic@stat.fsu.edu , kdy10@my.fsu.edu

Vladimir Balan
University Politehnica of Bucharest, Romania.
E-mail: vladimir.balan@upb.ro